ELSEVIER

Journal of Atmospheric and Solar-Terrestrial Physics 67 (2005) 1734–1743

Journal of ATMOSPHERIC AND SOLAR-TERRESTRIAL PHYSICS

www.elsevier.com/locate/jastp

Tracing magnetic helicity from the solar corona to the interplanetary space

M.L. Luoni[a,*], C.H. Mandrini[a], Sergio Dasso[a,b], L. van Driel-Gesztelyi[c,d,e], P. Démoulin[c]

[a]*Instituto de Astronomía y Física del Espacio, CONICET-UBA, CC. 67, suc. 28, 1428 Buenos Aires, Argentina*
[b]*Departamento de Física, Facultad de Ciencias Exactas y Naturales, UBA, 1428 Buenos Aires, Argentina*
[c]*Observatoire de Paris, LESIA, UMR 8109 (CNRS), F-92195 Meudon, Cedex, France*
[d]*Mullard Space Science Laboratory, University College London, Holmbury St. Mary, Dorking, Surrey, RH5 6NT, UK*
[e]*Konkoly Observatory, H-1525 Budapest, P.O. Box 67, Hungary*

Available online 30 August 2005

Abstract

On October 14, 1995, a C1.6 long duration event (LDE) started in active region (AR) NOAA 7912 at approximately 5:00 UT and lasted for about 15 h. On October 18, 1995, the Solar Wind Experiment and the Magnetic Field Instrument (MFI) on board the Wind spacecraft registered a magnetic cloud (MC) at 1 AU, which was followed by a strong geomagnetic storm. We identify the solar source of this phenomenon as AR 7912. We use magnetograms obtained by the Imaging Vector Magnetograph at Mees Solar Observatory, as boundary conditions to the linear force-free model of the coronal field, and, we determine the model in which the field lines best fit the loops observed by the Soft X-ray Telescope on board Yohkoh. The computations are done before and after the ejection accompanying the LDE. We deduce the loss of magnetic helicity from AR 7912. We also estimate the magnetic helicity of the MC from in situ observations and force-free models. We find the same sign of magnetic helicity in the MC and in its solar source. Furthermore, the helicity values turn out to be quite similar considering the large errors that could be present. Our results are a first step towards a quantitative confirmation of the link between solar and interplanetary phenomena through the study of magnetic helicity.

Keywords: Solar magnetic fields; Solar activity; Interplanetary magnetic clouds

1. Introduction

Coronal mass ejections (CMEs) are expulsions of mass and magnetic field from the Sun. Low (1996) pointed out that one of the most important roles of CMEs is to carry away magnetic helicity from the Sun, which would accumulate incessantly otherwise, since helicity generated by the dynamo, helical turbulence and the differential rotation does not change sign with the cycle. Magnetic helicity is defined for a field $\vec{B}$ within a volume V as: $H = \int_V \vec{A}.\vec{B}\,\mathrm{d}V$, where the vector potential $\vec{A}$ satisfies $\vec{B} = \vec{\nabla} \times \vec{A}$. On the northern hemisphere magnetic features have preferentially negative (left-handed) helicity, while the southern hemispheric features show preference for the opposite sign (positive, right-handed helicity; for a recent review see Pevtsov and Balasubramaniam, 2003). Since magnetic helicity is well preserved even in non-ideal MHD (Berger, 1984),

*Corresponding author. Tel.: +54 11 4783 2642; fax: +54 11 4786 8114.
E-mail address: mluoni@iafe.uba.ar (M.L. Luoni).

1364-6826/$ - see front matter
doi:10.1016/j.jastp.2005.07.003

the helicity is expected to be conserved during the ejection of a CME into the interplanetary space. Part of these ejections are detected in situ as magnetic clouds (MC). An MC is characterized by lower proton temperature and higher magnetic field strength than the surrounding solar wind. Typically, the magnetic field vector shows a smooth significant rotation across the cloud (Burlaga et al., 1981; Burlaga, 1990, 1995) indicating a helical (flux rope) magnetic structure, which clearly has non-zero helicity.

How much helicity is carried away from the Sun by a CME is still a question that may be answered by measuring the decrease of helicity in the solar corona due to a CME, or measuring the helicity content of the resulting MC. The first attempt to estimate the magnetic helicity of MCs was made by DeVore (2000), who used a sample of 18 MCs analyzed by Lepping et al. (1990). He obtained a mean helicity value of $2 \times 10^{42}\,\mathrm{Mx}^2$ (for a flux rope length of 0.5 AU) and a mean magnetic flux of 1×10^{21} Mx for these MCs. Démoulin et al. (2002) and Green et al. (2002) developed a method to measure the helicity content of active regions in the corona obtaining a typical value of $4\text{–}23 \times 10^{42}\ \mathrm{Mx}^2$. Building on DeVore's method for the estimation of the helicity content of MCs, they drew the helicity budget of two ARs from emergence through decay. They measured long-term (from one rotation to the next) changes in the coronal helicity content, identified all the CMEs ejected from the two ARs during their entire lifetime (31 and 66, respectively) and estimated the total amount of helicity ejected. However, they made no attempt to measure the decrease of coronal helicity due to any of these CMEs, nor they linked the CMEs to any in situ MC observation (see also Mandrini et al., 2004a).

Nindos et al. (2003) computed photospheric magnetic helicity influx (i.e. increase of coronal helicity) from foot-point motions using a local correlation tracking (LCT) method in six ARs prior to the occurrence of halo CME events. All these CMEs were linked to observed MCs. Using a flux-tube length determined by the condition for the initiation of the kink instability in the coronal flux rope for the MCs (which gives a length between of 0.6 and 1.3 AU), the helicities calculated were broadly consistent with the injection of helicity they obtained over 110–150 h time intervals prior to the CME events. However, the LCT method, as pointed out by Démoulin and Berger (2003), is likely to underestimate the photospheric magnetic helicity influx.

The first diagnostics of change in coronal helicity due to a CME was carried out by Bleybel et al. (2002). They used vector magnetograms prior to and after an eruptive event and a non-linear force-free magnetic field extrapolation code to compute the pre- and post-ejection helicities in the source region directly from the magnetograms, which were separated by 17.5 h. They found a helicity decrease of $0.7 \times 10^{42}\ \mathrm{Mx}^2$.

The first direct link between the measurement of magnetic helicity loss in the solar corona due to a CME and magnetic helicity computed in its resulting MC at 1 AU, was done by Mandrini et al. (2004b). Carrying out a multi-wavelength analysis of a sigmoidal coronal bright point, which appeared at Sun centre, they found evidence for its eruptive behavior (flaring followed by dimmings and the appearance of cusped loops). Using a linear force-free model of the pre- and post-eruption coronal loops they computed the change in coronal helicity due to the eruption (CME). Analyzing in situ data obtained by the Wind spacecraft, they found a small MC, which could be linked to the small solar eruption by timing, spatial magnetic orientation and field direction. Modeling the MC and having constraints on the length of its flux tube from the short lifetime of the solar source region, they calculated its helicity. The helicity change in the corona and the helicity content of the MC were the same: $3 \times 10^{39}\,\mathrm{Mx}^2$, which, given the unusually small size of the source region, can be regarded as a lower bound for the helicity loss due to a CME. However, we still lack such analysis for a more typical size CME/MC event.

On October 18–19, 1995, an MC reached the Earth producing an intense geomagnetic storm ($D_{st} = -120$ nT), the largest event observed in the period of 1994–1997. When the MC reached the Wind spacecraft, its magnetic field had a strong southward component ($-B_z$) for about 15 h, then the magnetic field vector turned northward for a period of about 15 h (see Fig. 3). Generally, a long time interval of negative B_z in a cloud causes geomagnetic disturbances, incoming particles, auroras, etc. Magnetic modeling of the observations showed that the cloud can be well approximated with a flux rope of right-handed twist (positive helicity, Lepping et al., 1997).

This MC was reportedly linked to a long-duration event (LDE) on the Sun by van Driel-Gesztelyi et al. (2000), a common low-coronal signature of CMEs. The coronal loops, observed in soft X-rays by Yohkoh/SXT Tsuneta et al. (1991), were highly sheared (sigmoidal) prior to the eruption; some loops were seen expanding during the flare and the AR loops became more potential a few hours after the flare maximum. The forward-S shape of the coronal loops suggested positive helicity, the same sign as was found in the corresponding MC.

This large geo-effective event, which was well observed both on the Sun and in the interplanetary (IP) space, provides a good opportunity for us to make the direct link between magnetic helicity change in the corona and the helicity observed at 1 AU. We describe the solar event and compute the change of helicity in the corona due to the CME (Section 2). In Section 3 we describe the IP event, model it and compute the magnetic helicity of the MC. Finally, in

Section 4 we discuss the results and in Section 5 we conclude.

2. The solar event on 14 October 1995

2.1. Sigmoid eruption

The source region, AR 7912, had a magnetic orientation opposite to Hale's Law (Fig. 1a). Based on the long-term (four rotations) evolution of the AR, it was proposed by López Fuentes et al. (2000) that AR 7912, having an opposite sign of twist and writhe, was formed by a helical flux tube which was deformed in the convection zone by external forces while ascending.

On 14 October a C1.6 (GOES class) LDE started in AR 7912 after ≈ 05:00 UT, reached maximum X-ray flux at 09:21 UT and lasted for at least 15 h. The LDE started by loop brightenings in the central part of the AR, during which some of the sigmoidal loops became visible. Expansion of coronal loops started at 05:23 UT. By 07:29 UT the expanding loops encountered the magnetic fields of neighboring regions and an "X-point" coronal structure appeared, presumably the result of inter-active-region reconnections (see Fig. 1b). The expansion of AR 7912 continued and by 08:22 UT (and certainly by 08:55 UT), the span of the fading loops, in projection, became comparable to the solar radius (see Fig. 1c). Similar sigmoid expansion was observed by Manoharan et al. (1996). For a more detailed description of the LDE we refer to van Driel-Gesztelyi et al. (2003).

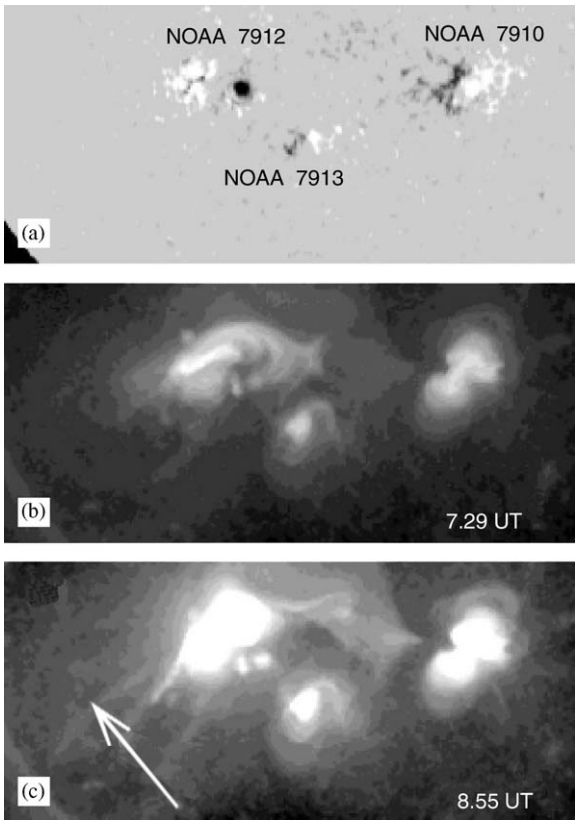

Fig. 1. (a) Kitt Peak magnetic map and (b,c) Yohkoh/SXT soft X-ray observations on 14 October 1995. (b) The highly sheared loops are in expansion in the X-ray image (taken before the peak of the LDE at 09:21 UT). Note the S-shaped loops in the reversed polarity AR 7912. (c) The dim huge loop (indicated by an arrow) seen in projection at 08:55 UT corresponds to the expanding sigmoid. Solar North is up and West to the right in these figures.

Since in October 1995 space-born coronagraph observations were not yet available, we do not have direct observation of the CME. However, a strong statistical link between LDE and CME occurrences (Webb, 1992) and the observation of the actually expanding sigmoidal structures provide evidence of a CME in this event.

2.2. Coronal magnetic helicity change

When a flux tube is ejected from the solar corona into the IP space, it carries away only a part of the magnetic helicity contained in the coronal field. Therefore, we need to compute the variation of the coronal magnetic helicity from before to after an eruptive event to estimate the ejected helicity.

To compute magnetic helicity in the corona, we first need to model the coronal field. Using magnetograms provided by the Imaging Vector Magnetograph (IVM) (Mickey et al., 1996; LaBonte et al., 1999), at Mees Solar Observatory, we have extrapolated the observed photospheric line of sight component of the field to the corona under the linear (or constant α) force-free field (fff) assumption: $\vec{\nabla} \times \vec{B} = \alpha \vec{B}$. Our code uses a fast Fourier transform method as proposed by Alissandrakis (1981), more details on the computation and the transformation of the observed field to heliographic coordinates can be found in Démoulin et al. (1997). Two different magnetograms from IVM were used to compute the coronal field, one at 00:20 UT and another at 17:55 UT, on October 14, 1995.

The only free parameter in a linear force-free field (lfff) model is the value of α. To determine α, we use two SXT full disk images, one at 07:30 UT (the time at which the SXT loops appeared to be most sheared) and the other at 11:58 UT (by this time the SXT loops became more relaxed). These times are well before the maximum of the LDE at 09:21 UT in GOES data and well after the largest observable expansion of the SXT loops (and maximum of the LDE), respectively. These SXT images are coaligned with the two previously mentioned IVM magnetograms. The value of α is determined through an

iterative process. First, we compute the coronal field assuming a given value for α; then, we determine the distance of the closest field-line for each observed SXT coronal loop and, finally, through successive computations with different α-values, we select the value of α that gives the best global fit either for a selected set of loops, or for the whole region (for more details see Green et al., 2002).

In general, α is not constant along the AR. In this particular case, α was higher in the northern part of the AR and lower in the southern part of AR 7912. This was the case for both magnetograms and SXT images chosen for our modeling. The values of α for the earlier magnetogram and SXT image are in the range of $(0.94–2.07)\times10^{-2}\,\mathrm{Mm}^{-1}$, while they are between $(0.12–1.50)\times10^{-2}\,\mathrm{Mm}^{-1}$ for the later magnetogram and coronal image. The field lines with the lower and higher α-values are shown in Fig. 2 with thin and thick lines.

Once the coronal model is determined, we compute the relative coronal magnetic helicity, H_{cor}, following Berger (1985). When α lies close to a critical value (α_{crit}), which depends on the size of the integration box, H_{cor} may take very high unphysical values (see the Appendix in Green et al., 2002). A way to avoid this artificial enhancement of H_{cor} for α close to α_{crit}, which is the case for our coronal model for SXT image at 07:30 UT, is to use a linearized version of the expression given by Berger (1985). We note that there were typographic errors in the published equation (Eq. (11) in Green et al., 2002); however, these typos appeared only in the script and did not influence the results. The correct expression is:

$$H_{\mathrm{cor}} = \alpha \sum_{n_x=0}^{N_x} \sum_{n_y=0}^{N_y} \frac{|\widetilde{B}^2_{n_x,n_y}|}{(k_x^2+k_y^2)^{3/2}}, \qquad (1)$$

where the mode $n_x = n_y = 0$ (uniform field) has no contribution. The use of this linearized expression implies that our helicity values, within the lfff approximation, represent a lower bound for the magnetic helicity value before the eruption (see Table 1). Furthermore, at the northern part of the AR (where the most sheared loops are observed) our model does not give a good representation of the coronal field because the observations do not include the magnetic field outside the AR (the IVM magnetograms cover only the AR magnetic field; then, our model cannot account for the connections towards AR 7910 at the East of AR 7912).

The coronal helicity results are shown in the third column of Table 1. The decrease of coronal magnetic helicity is in the range of $3\times10^{42}\,\mathrm{Mx}^2 \leqslant \Delta H_{\mathrm{cor}} \leqslant 6\times10^{42}\,\mathrm{Mx}^2$, giving an average of $\Delta H_{\mathrm{cor}} = 4.5\times10^{42}\,\mathrm{Mx}^2$.

3. The interplanetary event on 18–19 October, 1995

3.1. The magnetic cloud

The MC observed by the Wind spacecraft on October 18–19, 1995, has been studied by several authors (see e.g. Lepping et al., 1997; Larson et al., 1997; Janoo et al., 1998; Collier et al., 2001; Hidalgo et al., 2002). The in situ plasma and magnetic data indicate that the cloud reached the spacecraft at ~19:00 UT, on October 18, 1995. While the entry of the cloud is very clear, its exit time cannot be well determined and different authors take different values. An end time at ~23:00 UT, on October 19, 1995 has been taken by (Lepping et al., 1997; Janoo et al., 1998; Collier et al., 2001), which is the one we will use in this paper.

The orientation and the size of this cloud was determined by Lepping et al. (1997) and Hidalgo et al. (2002). The former authors fitted the physical parameters of the MC under the assumption of a lfff model for its magnetic configuration, while the latter ones used a non-force free constant current model.

Information on the length of the flux tube in MCs can be obtained by studying the electron distribution function. Counter-streaming electrons, when present, are considered to indicate magnetic connection to the Sun. The absence of electron streams is interpreted as a full disconnection. Based on such data, Larson et al. (1997) concluded that the October 18–19 MC was connected to the Sun at least at one end (see their Section 4 for a discussion). They estimated the semi-length of the magnetic field lines from in situ observations (at 1 AU) of impulsive electron events (~1–10^2 keV) and solar type III radio bursts. From an analysis of the arrival time of the electrons, the semi-length of the field lines near the centre of the cloud (i.e., lines practically parallel to the cloud axis) turned out to be ~1.2 AU, confirming that the flux tube was still connected to the Sun.

Here, we analyze the 1 min resolution magnetic data from the MFI aboard Wind. Our aim is to compute the magnetic flux and helicity content using two different approaches to determine the variation range of these magnitudes. The data were downloaded from http://cdaweb.gsfc.nasa.gov/cdaweb/istp-public/.

The magnetic structure of MCs is usually modeled by a cylindrical helix. To determine its orientation, we apply the minimum variance (MV) method to the data (see e.g. Bothmer and Schwenn, 1998). Then, we obtain the components of the field in a cartesian system attached to the cloud (local components), such that: (a) $B_{z,\mathrm{cloud}}$ is the axial component, being its value positive at the cloud centre, (b) $B_{y,\mathrm{cloud}}$ is the poloidal component once the spacecraft crossed its axis, and (c) $B_{x,\mathrm{cloud}}$ is the radial component, also after leaving the

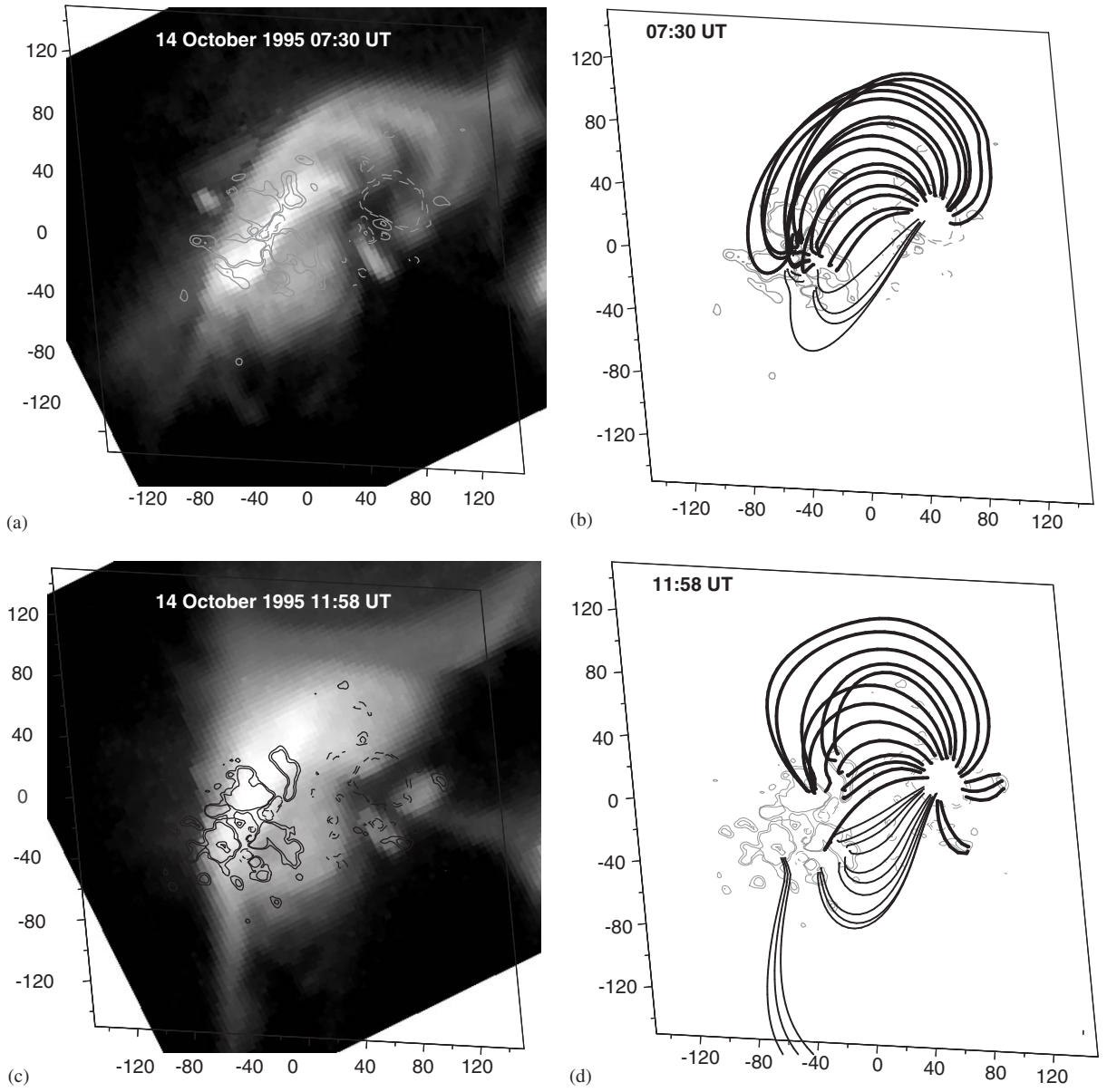

Fig. 2. Yohkoh/SXT soft X-ray images overlaid with longitudinal magnetograms (left) and coronal linear force-free model (right) of AR 7912. Isocontours (±70, ±140G) are drawn with continuous/dashed lines for positive/negative magnetic field values. The scale of the vertical and horizontal axes is in Mm. Terrestrial North is up in the magnetic data, the coronal images have been rotated accordingly.

MC centre. Fig. 3 shows the components of the magnetic field in an extended range of time. Dashed lines mark the two boundaries of the cloud.

3.2. Magnetic cloud model

Several modeling and fitting methods have been used to reproduce the magnetic structure of MCs; however, it is not yet clear which one is the best to describe it. We model the cloud field using two fff configurations: (1) a lfff (model L, Lundquist, 1950), and (2) a non-linear fff with uniform twist (model GH, Gold and Hoyle, 1960). Using the MV coordinates, we compare the observations with the results for the two models. The physical parameters that best fit the observations are computed following the method described in Dasso et al. (2003). The radius of the cloud is estimated from the duration of the MC and the observed solar

Table 1
Left block of columns shows the time, the range of the lfff parameter α, and the range of the AR relative magnetic helicity H_{cor}

Active region			Magnetic cloud		
Time (UT)	α (10^{-2} Mm^{-1})	H_{cor} (10^{42} Mx^2)	Model	F (10^{21} Mx)	H_{MC} (10^{42} Mx^2)
07:30	0.94–2.07	7–15	L	1.1	9
11:58	0.12–1.50	1–12	GH	1.2	8

Right block shows the model name, the computed axial flux (F) and relative magnetic helicity of the MC, H_{MC}, computed for a length of 2.4 AU.

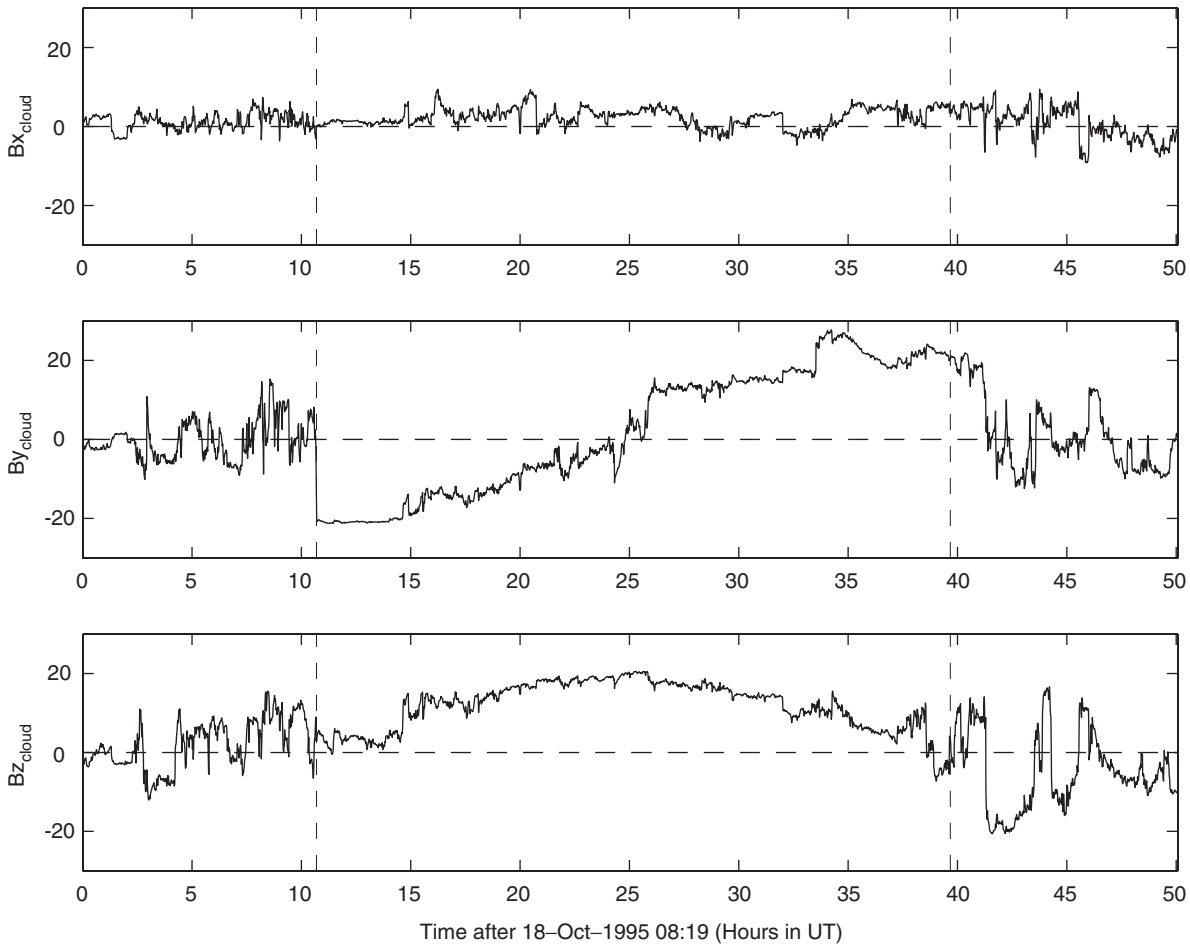

Fig. 3. Interplanetary magnetic field (in local components) of the MC. Dashed lines show the boundaries of the cloud.

wind speed. The curves from the two models, together with the observations are shown in Fig. 4 for $B_{z,\mathrm{cloud}}$ and $B_{y,\mathrm{cloud}}$.

From the models, we deduced an axial flux $F \approx 1.15 \times 10^{21}$ Mx for the MC (Table 1). At least three sets of MCs, analyzed with model L, have been published: 18 MCs by Lepping et al. (1990), 23 MCs by Zhao et al. (2001) and 28 MCs by Watari et al. (2001). The average values of the axial magnetic field B_0 are $(2, 2.4, 1.8) \times 10^{-4}$ G and the values of the radius are $(2.1, 1.7, 1.5) \times 10^{12}$ cm, respectively. The lfff model then gives axial-flux values of $(1.3, 1.1, 0.7) \times 10^{21}$ Mx, respectively. So the value of F found (Table 1) is comparable to the mean flux found within three sets of MCs. This value corresponds to $\approx 10\%$ of the total flux of AR 7912.

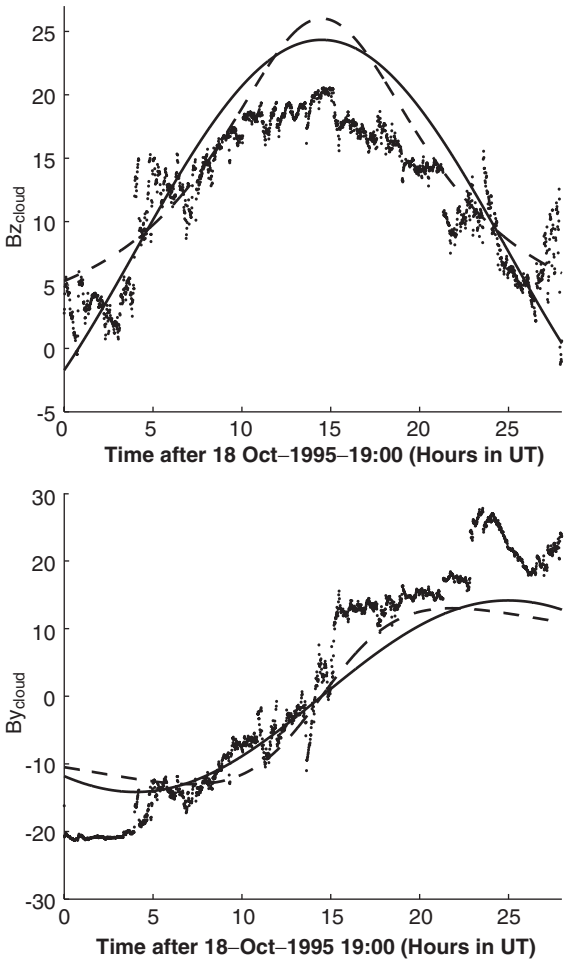

Fig. 4. $B_{z,\mathrm{cloud}}$ (top) and $B_{y,\mathrm{cloud}}$ (bottom) components of the interplanetary magnetic field. Dots correspond to the observed field, while the solid and dashed lines show the result of the fitting to Lundquist and Gold–Hoyle models, respectively.

A gauge-invariant relative magnetic helicity (H_{MC}) has been deduced by Dasso et al. (2003) for the two models (L and GH) used here. Following their computations, we quantify H_{MC} from the fitted parameters using a flux tube length of 2.4 AU. The results of the two models are comparable (Table 1) and are a factor two larger than the helicity change found at the coronal level (Section 2.2). We further discuss the helicity results in the next section.

4. Discussion

The decrease of the coronal helicity due to the eruption was analyzed previously by Bleybel et al. (2002) using the same IVM vector magnetograms as we used. They obtained a decrease of $0.7 \times 10^{42}\,\mathrm{Mx}^2$, a factor of six lower than our value ($4.5 \times 10^{42}\,\mathrm{Mx}^2$). A non-linear force-free field (nlfff) model of the coronal field, utilized by Bleybel et al., is generally considered superior to the lfff approximation utilized by us, since the nlfff approach allows for local (even sign) changes in α, while in the lfff approach α is uniform. Since photospheric electric currents are observed to be concentrated and patchy, the former approach is certainly more realistic. However, the nlfff computations use the transverse field measurements to derive the current density. It is presently difficult to compute reliable photospheric currents over a full AR, in particular because of the noise level in the transverse field and the difficulty to resolve the 180° ambiguity (see e.g. Gary and Démoulin, 1995). The nlfff numerical methods have also their own problems and the result of different methods still needs to be compared. Moreover, since the total magnetic flux reported in Table 1 of Bleybel et al. ($8.4–7.3 \times 10^{25}\,\mathrm{cm}^2\,\mathrm{G}$, or Mx) appears to be four orders of magnitude higher than that of solar active regions (we measured a total flux of $7.8–8.4 \times 10^{21}$ Mx on the same magnetograms), the validity of their reported helicity values, which are also one order of magnitude lower than the helicity found by us in the related MC, may raise questions.

How accurate is the helicity change in the corona we obtained? We are confident that we have found the right order of magnitude, since this order is confirmed by the independent estimation in the MC. However, it is extremely difficult to estimate an error for the computed helicity because the observed coronal field is not fully relaxed to a linear force-free state. The general property of a lfff is to make the shorter (resp. longer) field lines less (resp. more) sheared than the observed coronal loops. This implies that the lfff has very low (resp. too large) magnetic helicity in the small scales (resp. large scales) compared to the coronal field (see e.g. Schmieder et al., 1996). Since the value of α is selected so that the lfff represents the best global fit to the observed coronal loops, we hope that the over/under estimate of helicity at large/small scales roughly compensate each other. However, this can only be verified when another method will be available to estimate the coronal helicity.

Several works have estimated the magnetic helicity content in MCs. DeVore (2000) computed the relative helicity in an MC using Berger's (1999) equation, and the average values of the axial magnetic field B_0 and radius R for a set of 18 clouds studied by Lepping et al. (1990). We have done the same computation for the sets analyzed by Zhao et al. (2001) and Watari et al. (2001). The mean helicity per unit length along the MC, $\mathrm{d}H/\mathrm{d}l$, is $(4.9, 5.6, 2.2) \times 10^{42}\,\mathrm{Mx}^2$ for the three sets, respectively. Nindos and Zhang (2002) found that $\mathrm{d}H/\mathrm{d}l$ of an MC was as large as $64 \times 10^{42}\,\mathrm{Mx}^2$. However, taking the average of MCs observed in the year 2000 they obtained

an average value of $dH/dl \approx 8 \times 10^{42}\,Mx^2$. In another paper, Nindos et al. (2003), using observations of MCs ejected from 6 ARs via halo CMEs, found dH/dl in the range of $[1.5, 15] \times 10^{42}\,Mx^2$. As a counterpart to these large MCs, Mandrini et al. (2004b) identified an ejection and associated very small MC for which they estimated $dH/dl \approx 3 \times 10^{39}\,Mx^2$. In summary, the helicity content of MCs determined so far are between the orders of 10^{39}–$10^{43}\,Mx^2$, with a mean of about a few times of $10^{42}\,Mx^2$.

As for the geo-effective MC of October 18–19, there are several uncertainties in our magnetic helicity estimation. On one hand, there is still no consensus over the flux tube length of the MC, which enters as a multiplicative factor in the helicity value. According to Larson et al. (1997) the semi-length of the field lines at the center could be estimated as 1.2 AU in at least one leg of the MC (see Section 3.1), but these authors note that the heat flux of energetic electrons presented numerous abrupt changes, from bi-directional streaming to unidirectional streaming to complete disappearance, implying a patchy magnetic disconnection from the Sun of one or possibly even both ends. Then, the value of H_{MC} using a length of 2.4 AU is an upper limit for the cloud helicity, since we cannot ascertain that the 1.2 AU length applies to both cloud legs.

All the helicity studies (including the present one) have considered that the cross-section of MCs is circular (see references in Section 3.1). However, if the cross-section shape is oblate instead, then, our helicity values could be underestimated (see Vandas and Romashets, 2003, for a generalization of the Lundquist model to an oblate structure). This is likely to be the case in the studied MC since the observed norm of the magnetic field is more uniform across the section than in the cylindrical models. Furthermore, since the magnetic helicity value depends strongly on the radius (to the fourth power, see Dasso et al., 2003) any uncertainty in its determination influences the results. We have computed our radius taking the cloud end time at 23:00 UT on October 19, 1995, other authors (Larson et al., 1997; Hidalgo et al., 2002) have taken the cloud end time at ≈ 01:40 UT on 20 October. Extending our end time to the latter would also imply a larger MC helicity value. Another uncertainty comes from the unknown distribution of the twist along the interplanetary flux rope, whether it is uniform or not. We assume that the twist is uniformly distributed. As at the coronal level, only future research will be able to test the precision of this approach.

Leamon et al. (2004) derived the axial magnetic flux, the total current, and the field line twist (number of turns) from in situ observations of 12 MCs and compared these properties with those of the corresponding ARs. The aim of this work was to find the origin of the magnetic flux and twist in the MCs. They found that the axial magnetic flux of an MC is comparable to the magnetic flux of its associated AR; while we rather find a factor 10 times lower flux in the MC, in agreement with our previous studies (Démoulin et al., 2002; Green et al., 2002; Mandrini et al., 2004b) and also with the results by Nindos et al. (2003). Leamon et al. also found that there is no statistically significant sign relationship between the magnetic twist measured in an MC and its related AR, again a result different from previous studies (e.g. Rust, 1994; Nindos et al., 2003; Pevtsov and Balasubramaniam, 2003). They also concluded, in agreement with earlier studies, that the magnetic field in MCs is much more twisted (≈10 turns end to end) than that of the related ARs, and that the twist is created through magnetic reconnection during the eruption. We agree on this point. Magnetic reconnection can indeed create a high number of turns from a sheared arcade (Berger, 1998), while it preserves the total magnetic helicity; so the helicity lost from the corona is expected to appear in the IP space. Therefore, our finding that the helicity change in the AR is comparable with the MC helicity is fully compatible with a higher twist in the MC than in its solar source region.

5. Conclusion

We computed the relative magnetic helicity in AR 7912 before and after the ejection that accompanied a C1.6 LDE, which occurred on October 14, 1995, in order to obtain the helicity carried away by the CME. We also computed the helicity content of the well-observed MC of October 18–19, 1995, which was reportedly related to the solar event.

In spite of all the uncertainties involved both in the solar and interplanetary modeling, the coronal and MC helicity values we obtained: (i) have the same sign (>0) and (ii) their magnitudes agree within a factor of two ($4.5 \times 10^{42}\,Mx^2$ in the corona and $8.5 \times 10^{42}\,Mx^2$ for the MC). The close correspondence of these values, obtained independently, based on remote sensing and in situ data and different modeling methods, is very promising. Therefore, we conclude that the CME ejected from the Sun on 14 October, 1995, carried away magnetic helicity of a few times $10^{42}\,Mx^2$.

Acknowledgements

We thank the NASA's Space Physics Data Facility (SPDF), the MSSL/SURF for YOHKOH/SXT and Mees Solar Observatory, University of Hawaii, for their data. This work was partially supported by the Argentinean grants: UBACyT X329, PIP 2693 and PIP 2388 (CONICET), and PICT 12187 (ANPCyT). L. v. D. G. was supported by the Hungarian Government

grant OTKA T-038013. C. H. M. and P. D. thank ECOS (France) and SECyT (Argentina) for their cooperative science program A01U04. C. H. M. and L. v. D. G. acknowledge TET (Hungary) and SECyT for financial support through their cooperative program (AR03/02 and HU/A01/UIII/01). C. H. M. and S. D. are members of the Carrera del Investigador Científico, CONICET.

References

Alissandrakis, C.E., 1981. On the computation of constant alpha force-free magnetic field. Astronomy and Astrophysics 100, 197–200.

Berger, M.A., 1984. Rigorous new limits on magnetic helicity dissipation in the solar corona. Geophysical and Astrophysical Fluid Dynamics 30, 79–104.

Berger, M.A., 1985. Structure and stability of constant-alpha force-free fields. Astrophysical Journal Supplement Series 59, 433–444.

Berger, M.A., 1998. Magnetic helicity and filaments. Astronomical Society of the Pacific Conference Series 150, 102–110.

Berger, M.A., 1999. Magnetic Helicity in Space Physics. Magnetic Helicity in Space and Laboratory Plasmas, Geophysical Monograph, vol. 111, AGU, Washington DC, pp. 1–9.

Bleybel, A., Amari, T., van Driel-Gesztelyi, L., Leka, K.D., 2002. Global budget for an eruptive active region. I. Equilibrium reconstruction approach. Astronomy and Astrophysics 395, 685–695.

Bothmer, V., Schwenn, R., 1998. The structure and origin of magnetic clouds in the solar wind. Annales Geophysicae 16, 1–24.

Burlaga, L.F., 1990. Magnetic clouds. Physics of the Inner Heliosphere, vol. II, Springer, Berlin, pp. 1–22.

Burlaga, L.F., 1995. Interplanetary Magnetohydrodynamics. Oxford University Press, New York.

Burlaga, L.E., Sittler, F., Mariani, F., Schwenn, R., 1981. Magnetic loop behind an interplanetary shock—Voyager, Helios, and IMP 8 observations. Journal of Geophysical Research 86, 6673–6684.

Collier, M.R., Szabo, A., Farrell, W.M., Slavin, J.A., et al., 2001. Reconnection remnants in the magnetic cloud of October 18–19, 1995: a shock, monochromatic wave, heat flux dropout, and energetic ion beam. Journal of Geophysical Research 106 (A8), 15,985–16,000.

Dasso, S., Mandrini, C.H., Démoulin, P., Farrugia, C.J., 2003. Magnetic helicity analysis of an interplanetary twisted flux tube. Journal of Geophysical Research 108 (A10), DOI 10.1029/2003JA009942.

Démoulin, P., Berger, M.A., 2003. Magnetic energy and helicity fluxes at the photospheric level. Solar Physics 215, 203–215.

Démoulin, P., Bágala, L.G., Mandrini, C.H., Hénoux, J.C., Rovira, M.G., 1997. Quasi-separatrix layers in solar flares. II. Observed magnetic configurations. Astronomy and Astrophysics 325, 1213–1225.

Démoulin, P., Mandrini, C.H., van Driel-Gesztelyi, L., Thompson, B.J., Plunkett, S., et al., 2002. What is the source of the magnetic helicity shed by CMEs? The long-term helicity budget of AR 7978. Astronomy and Astrophysics 382, 650–665.

DeVore, C.R., 2000. Magnetic helicity generation by solar differential rotation. Astrophysical Journal 539, 944–953.

Gary, G.A., Démoulin, P., 1995. Reduction, analysis and properties of electric current systems in solar active regions. Astrophysical Journal 445, 982–998.

Gold, T., Hoyle, F., 1960. On the origin of solar flares. Monthly Notices of the Royal Astronomical Society 120, 89–105.

Green, L.G., López-Fuentes, M.C., Mandrini, C.H., Démoulin, P., van Driel-Gesztelyi, L., Culhane, J.L., 2002. The magnetic helicity budget of a CME-prolific active region. Solar Physics 208, 43–68.

Hidalgo, M.A., Cid, C., Viñas, A.F., Sequeiros, J., 2002. A non-force-free approach to the topology of magnetic clouds in the solar wind. Journal of Geophysical Research 107 (A1), DOI 10.1029/2001JA900100.

Janoo, L., Farrugia, C.J., Torbert, R.B., Quinn, J.M., Szabo, A., 1998. Field and flow perturbations in the October 18–19, 1995, magnetic cloud. Journal of Geophysical Research 103 (A8), 17,261–17,278.

LaBonte, B.J., Mickey, D.L., Leka, K.D., 1999. The Imaging Vector Magnetograph at Haleakala—II. Reconstruction of Stokes spectra. Solar Physics 189, 1–24.

Larson, D.E., Lin, R.P., McTiernan, J.M., McFadden, J.P., Ergun, R.E., et al., 1997. Tracing the topology of the October 18–20, 1995, magnetic cloud with 0.1–102 keV electrons. Geophysical Research Letters 24, 1911–1914.

Leamon, R.J., Canfield, R.C., Jones, S.L., Lambkin, K., Lundberg, B.J., Pevtsov, A.A., 2004. Helicity of magnetic clouds and their associated active regions. Journal of Geophysical Research 109 (A5), DOI 10.1029/2003JA010324.

Lepping, R.P., Burlaga, L.F., Jones, J.A., 1990. Magnetic field structure of interplanetary magnetic clouds at 1 AU. Journal of Geophysical Research 95, 11,957–11,965.

Lepping, R.P., Burlaga, L.F., Szabo, A., Ogilvie, K.W., Mish, W.H., et al., 1997. The Wind magnetic cloud and events October 18–20, 1995: interplanetary properties and as triggers for geomagnetic activity. Journal of Geophysical Research 102 (A7), 14,049–14,063.

López Fuentes, M.C., Démoulin, P., Mandrini, C.H., van Driel-Gesztelyi, L., 2000. The counterkink rotation of a non-hale active region. Astrophysical Journal 544, 540–549.

Low, B.C., 1996. Solar activity and the corona. Solar Physics 167, 217–265.

Lundquist, S., 1950. Magnetohydrostatic fields. Arkiv for Fysik 2, 361–365.

Mandrini, C.H., Démoulin, P., van Driel-Gesztelyi, L., Green, L.M., López Fuentes, M.C., 2004a. Magnetic helicity budget of solar-active regions from the photosphere to magnetic clouds. Astrophysics and Space Science 290, 319–344.

Mandrini, C.H., Pohjolainen, S., Dasso, S., Green, L.M., Démoulin, P., van Driel-Gesztelyi, L., Copperwheat, C., Foley, C., 2004b. Interplanetary flux rope ejected from and X-ray bright point. The smallest magnetic cloud source region ever observed. Astronomy and Astrophysics, submitted.

Manoharan, P.K., van Driel-Gesztelyi, L., Pick, M., Démoulin, P., 1996. Evidence for large-scale solar magnetic reconnec-

tion from radio and X-ray measurements. Astrophysical Journal 468, L73–76.

Mickey, D.L., Canfield, R.C., Labonte, B.J., Leka, K.D., Waterson, M.F., Weber, H.M., 1996. The Imaging Vector Magnetograph at Haleakala. Solar Physics 168, 229–250.

Nindos, A., Zhang, H., 2002. Photospheric motions and coronal mass ejection productivity. Astrophysical Journal 573, L133–L136.

Nindos, A., Zhang, J., Zhang, H., 2003. The magnetic helicity budget of solar active regions and coronal mass ejections. Astrophysical Journal 594, 1033–1048.

Pevtsov, A.A., Balasubramaniam, K.S., 2003. Helicity patterns on the Sun. Advances in Space Research 32 (10), 1867–1874.

Rust, D.M., 1994. Spawning and shedding helical magnetic fields in the solar atmosphere. Geophysical Research Letters 21, 241–244.

Schmieder, B., Démoulin, P., Aulanier, G., Golub, L., 1996. Differential magnetic field shear in an active region. Astrophysical Journal 467, 881–886.

Tsuneta, S., Acton, L., Bruner, M., Lemen, J., Brown, W., et al., 1991. The soft X-ray telescope for the SOLAR-A mission. Solar Physics 136, 37–67.

Vandas, M., Romashets, E.P., 2003. A force-free field with constant alpha in an oblate cylinder: a generalization of the Lundquist solution. Astronomy and Astrophysics 398, 801–807.

van Driel-Gesztelyi, L., Manoharan, P.K., Démoulin, P., Aulanier, G., Mandrini, C.H., et al., 2000. Initiation of CMEs: the role of magnetic twist. Journal of Atmospheric and Solar-Terrestrial Physics 62 (16), 1437–1448.

van Driel-Gesztelyi, L., Démoulin, P., Mandrini, C.H., 2003. Observations of magnetic helicity. Advances in Space Research 32 (10), 1855–1866.

Watari, S., Watanabe, T., Marubashi, K., 2001. Soft X-ray solar activities associated with interplanetary magnetic flux ropes. Solar Physics 202, 363–384.

Webb, D.F., 1992. The solar sources of coronal mass ejections. In: Svestka, Z., Jackson, B.V., Machado, M.E. (Eds.), Eruptive Solar Flares. Springer, Berlin, pp. 234–247.

Zhao, X.P., Hoeksema, J.T., Marubashi, K., 2001. Magnetic cloud B_s events and their dependence on cloud parameters. Journal of Geophysical Research 106, 15,643–15,656.